Role of lubricated contacts in concentrated polydisperse suspensions

Christophe Ancey[a)]

Cemagref, 2 rue de la Papeterie, B.P. 76, 38402 Saint-Martin d'Hères Cedex, France

(Received 13 December 2000; final revision received 17 August 2001)

Synopsis

In this article experimental results of the bulk behavior of concentrated suspensions of coarse and fine (colloidal) particles in a Newtonian fluid (water) are presented. Different rheological behaviors can be observed depending on both the solid concentrations in fine and coarse particles and the shear velocity. For suspensions concentrated in coarse particles that are poor in fine particles, the bulk behavior is frictional for low shear velocities and viscous for sufficiently large shear velocities. In the converse case, for mixtures rich in fine particles, the bulk behavior is viscoplastic. A more complex time-dependent behavior can be observed when the viscoplastic force exerted by the dispersion on coarse particles roughly balances the force of gravity. The diversity in bulk behavior is explained by the specific role played by the contact between coarse particles. © *2001 The Society of Rheology.* [DOI: 10.1122/1.1413504]

I. INTRODUCTION

In physics of particle suspensions, attention has been drawn mainly to monodisperse suspensions [Coussot and Ancey (1999); Jomha *et al.* (1990)]. In some cases in which polydispersity was addressed, authors considered that the particle-size distribution can be conveniently replaced by a mean diameter. Such an approximation is expected to be reliable as soon as almost all the particles have the same kind of interaction. A typical example of treatment is given in the model of Zhou *et al.* (1999) which focuses on colloidal dispersions with a narrow particle-size distribution. In the converse case in which two or more types of interaction control the particle dynamics, this approximation no longer holds.

The first step in modeling polydisperse suspensions is to consider as many size grades as there are different types of particle interaction. However, in most cases encountered in civil engineering and the environment, suspensions usually involve broad particle-size distributions and Newtonian interstitial fluids. In this case, there are many different types of particle interaction depending on the particle size, shear rate, solid concentration, and temperature [Coussot and Ancey (1999)]: Brownian effects, colloidal surface forces (electrostatic attractive forces and van der Waals attractive forces), viscous forces, and contact forces (lubrication, solid friction, collision). Therefore, in the general case, determining the chief interactions within a suspension with a wide size distribution is difficult. Here we examine a limiting case of very concentrated suspensions with a bimodal size distribution. Contrary to other authors who investigated the properties of concentrated

[a)]Electronic mail: christophe.ancey@cemagref.fr

polydisperse suspensions with a continuous particle-size distribution, we have preferred to consider a bimodal distribution which is much easier to understand. The fine fraction is made up of colloidal particles whereas the coarse fraction includes large noncolloidal non-Brownian particles. For very concentrated suspensions of coarse particles, interactions between particles are generally the key process in bulk stress generation. This is clearly shown in the case of concentrated suspensions of coarse particles within Newtonian fluids but, as far as we know, the question has rarely been debated for bimodal suspensions and thus remains unresolved. The main objective of this article is to delineate the different rheological behaviors of such suspensions according to relevant dimensionless groups.

With this purpose in mind, we report the investigation of the effects of the solid concentration in the fine fraction on the bulk behavior of a concentrated suspension. First we will review different work and interpretations on the rheology of polydisperse suspensions (including fine and coarse particles). Dimensional analysis can be helpful in identifying the chief flow regimes and relevant dimensionless groups governing bulk behavior. Here extend the approach to bimodal suspensions by introducing dimensionless numbers defined as ratios of interparticle forces to the buoyant force. We will then present the rheometrical device (vane shear cell) and the procedures used in our experiments. Section V is devoted to our experimental results.

II. PREVIOUS EXPERIMENTAL RESULTS AND INTERPRETATION

In their study of coal slurries, Wildemuth and Williams (1984, 1985) found that, when the solid concentration exceeded a critical value, a polydisperse suspension exhibited yield stress, which reflects either colloidal effects or structural changes in the particle arrangement (jamming, friction between coarse particles) or both. Further experimental evidence of yielding behavior has been clearly reported by Husband *et al.* (1993) for noncolloidal systems (polyisobutylene/calcium carbonate suspensions). They also observed that, for solid concentrations in excess of a critical value ($\phi \approx 0.47$), suspensions exhibited yield stress. Moreover, this yield stress increased dramatically when the solid concentration came closer to the maximum concentration. In this case, the authors attributed yielding behavior either to particle jams or weak polymer–particle interactions. Such behavior was also observed by Kytömaa and Prasad (1993) with 2 mm glass beads in a water–glycerol solution, by Coussot (1997) with 100 μm polystyrene beads in water–glycerol solutions, and by Jomha *et al.* (1990) with 2 μm polystyrene beads in water.

The first insight into the physics of polydisperse suspensions was provided by Sengun and Probstein (1989) in their investigations on the viscosity of coal slurries. They proposed two approximations. First, as it is the interstitial phase, the dispersion resulting from the mixing of fine colloidal particles and water imparts most of its rheological properties to the entire suspension, notably its viscoplastic properties. Second, the coarse fraction is assumed to act independently of the fine fraction and to enhance the bulk viscosity. Experiments on viscosity of coal slurries performed by Sengun and Probstein (1989) confirmed the reliability of this concept, except that, for solid concentrations in the coarse fraction exceeding 0.35, they observed a significant change in behavior that they ascribed to nonuniformity in the shear-rate distribution within the bulk due to squeezing effects between coarse particles. Other authors have confirmed that the bulk yield stress in a suspension of coarse and fine colloidal particles depends on the coarse fraction in a more drastic way than predicted by Sengun and Probstein's model. Typical

examples include the experiments performed by Coussot and Piau (1995) on sand suspensions in a natural mud dispersion as well as by Banfill (1994, 1999) on concrete.

More recently, Mansoutre (2000) and Mansoutre *et al.* (1999) has contributed further elements showing the increasing importance of the coarse fraction in concentrated polydisperse systems. In her rheological study of tricalcic silicate, she found that, at low and intermediate concentrations, yield stress resulted from colloidal interactions since it was linearly dependent on the ionic strength. When the solid concentration exceeded a critical value, the yield stress increased much more rapidly and a nonzero normal stress appeared. She interpreted this to be result of ''*dilatant behavior*.'' Moreover, as the increment in yield stress produced by this phenomenon was to a large extent a linear function of the normal stress, she inferred that, at high concentrations, bulk yield stress resulted from both colloidal and frictional interactions.

III. PHYSICAL BACKGROUND AND NOTATION

Expressing bulk behavior in terms of dimensionless groups is the practical and usual way of identifying the most relevant variables and delineating flow regimes. A number of studies have so far focused on suspensions of rigid spherical particles within a Newtonian fluid with a narrow size distribution [Coussot and Ancey (1999); Jomha *et al.* (1990); Krieger (1972); Russel, Saville, and Schowalter (1995)]. It has been shown that, for a coarse-particle suspension of radius a and density ρ_p within a Newtonian fluid of viscosity η_0, bulk viscosity mainly depends on the solid concentration: $\eta = \eta(\phi)$, where ϕ denotes the solid volume concentration. For a dispersion, it also depends on the Péclet number: $\eta = \eta(\phi, Pe)$, where the Péclet number is expressed as $Pe = 6\pi\dot{\gamma}a^3\eta_0/(kT)$, where k refers to the Boltzmann constant, T is the temperature, and $\dot{\gamma}$ is the shear rate [Russel (1980); van der Werff and de Kruif (1989)].

In the present context, we have two populations of particles (fine and coarse particles). Using dimensional analysis arguments, it can be shown that a bimodal suspension possesses at least 10 degrees of freedom (or dimensionless groups). This should make intricate any thorough examination of the resulting flow regimes. In the present article, where attention is focused on highly concentrated suspensions, the question arises as to which dimensionless numbers can be discarded and therefore how many regimes can be determined. A scrutiny of the usual dimensionless numbers (particle Reynolds number, Stokes number, etc.) is not very helpful because they do not reflect the actual physics of concentrated bimodal suspensions. Indeed, concentrated unimodal suspensions differ from dilute suspensions through two major features. First, bulk behavior is chiefly dictated by particle–particle interactions (collision, lubricated contacts, friction, colloidal forces, etc.) and therefore further mechanisms (thereby dimensionless groups) must be taken into account [Coussot and Ancey (1999)]. Second, for solid concentrations exceeding a critical value similar to a dynamical percolation yield, a continuous network of particles in contact forms throughout the bulk, causing significant changes in flow behavior: dilatancy, ordering of particles in layers (for simple shear flows), rearrangement of stress components, the appearance of a minimum in the flow curve, and so on.

The particulate contribution to bulk stress in a suspension may be computed as the volume or ensemble average of interaction forces $\mathbf{f}$ between particles, whatever the type of interaction [Ancey *et al.* (1999b); Jongshaap and Mellema (1995)]: $\boldsymbol{\sigma} = n_d\langle \mathbf{f}\otimes\mathbf{r}\rangle$, where $\mathbf{r}$ denotes the distance between the mass centers of two interacting particles and n_d is the number density. Here, since we have two populations of grains (colloidal and coarse particles), we can express the particulate contribution to bulk stress as follows: $\boldsymbol{\sigma} = \phi_k(1-\phi_c)\boldsymbol{\sigma}_{\text{col}} + \phi_c\boldsymbol{\sigma}_{\text{coarse}}$, where $\boldsymbol{\sigma}_{\text{col}} = \langle \mathbf{f}\otimes\mathbf{r}\rangle/V_p$ and $\boldsymbol{\sigma}_{\text{coarse}} = \langle \mathbf{f}\otimes\mathbf{r}\rangle/V_p$ are

the elementary contributions of colloidal and coarse particles, respectively, both calculated on a test particle (of volume V_p). We use the subscript k to refer to kaolin properties. The solid concentration in kaolin is defined with respect to the water volume V_w: $\phi_k = V_k/(V_k+V_w)$, where V_k denotes the kaolin volume. Likewise, the subscript c refers to the coarse particles. The solid concentration in the coarse fraction ϕ_c is defined with respect to the total interstitial phase volume V_i: $\phi_c = V_c/(V_c+V_i)$, where V_c denotes the coarse-particle volume.

In the case of coarse particles in a Newtonian fluid, the (squeezing) lubrication force $\mathbf{f}$ between two particles separated by a distance ϵa (with $\epsilon \ll 1$) is proportional to their relative velocity U: $|\mathbf{f}| = 3\pi\eta_0 a U/(2\epsilon)$. In this case, in most existing theories it is found that the bulk behavior is Newtonian, with bulk viscosity defined as a function of the solid concentration [van den Brule *et al.* (1991)]. In the case of colloidal particles in a Newtonian fluid, the particle interactions $\mathbf{f}$ results from van der Waals' attractive forces and electrostatic repulsive forces. Due to the complexity of these surface forces, the resulting stress tensor $\boldsymbol{\sigma}_{\text{col}}$ can be computed only for certain cases. In the present context, we are mainly interested in weakly aggregated dispersions, where the van der Waals forces are more dominant than electrostatic forces. Kapur *et al.* (1997), Scales *et al.* (1998), then Zhou *et al.* (1999) have shown that bulk behavior is viscoplastic and close to the isoelectric point, and the maximum yield stress can be written over a wide range of solid concentrations as

$$\tau_k(\phi_k) = \kappa\left(\frac{\phi_k}{1-\phi_k}\right)^c \frac{1}{(2a_k)^2}, \tag{1}$$

where $\kappa = 3.1Ab/(24\pi\epsilon a)$, A is the Hamaker constant of the colloidal particles, b and c are two parameters to be fitted from experimental data, and a_k is the average diameter of the fine fraction.

To evaluate the strength of the squeezing effect, we can define a dimensionless number Γ_a by dividing the squeezing force by the buoyant force experienced by a test particle. By considering the case in which the fluid pressure is hydrostatic, we infer that the buoyant force is $4\rho' g \pi a^3/3$, where $\rho' = \phi(\rho_p-\rho_f)$ is called the buoyant density. We find

$$\Gamma_a = \frac{9}{8}\frac{1}{\epsilon}\frac{\eta_0 U}{\rho' g a^2}. \tag{2}$$

In very concentrated suspensions, a network of particles in direct contact occurs, the gravity force is transmitted through the different layers such that, at a depth h, a particle experiences an average "effective" normal stress $\rho' g h$ [Terzaghi (1943)]. In this case, the corresponding dimensionless number is

$$\Gamma = \frac{9}{4}\frac{a}{\epsilon}\frac{\eta_0 \dot{\gamma}}{\rho' g h}. \tag{3}$$

Several experiments have shown that Γ is the relevant dimensionless number in the behavior of concentrated suspensions when particles come into close contact. For instance, Acrivos and co-workers (1993) have demonstrated that the viscous resuspension of an initially settled bed of particules is controlled by Γ. Likewise Ancey and Coussot (1999a) have shown that Γ could scale the flow curves for suspensions of heavy particles within a Newtonian fluid. Figure 1 is a log–log plot of the shear stress against the shear velocity, combining some of their experimental data and one series of data presented

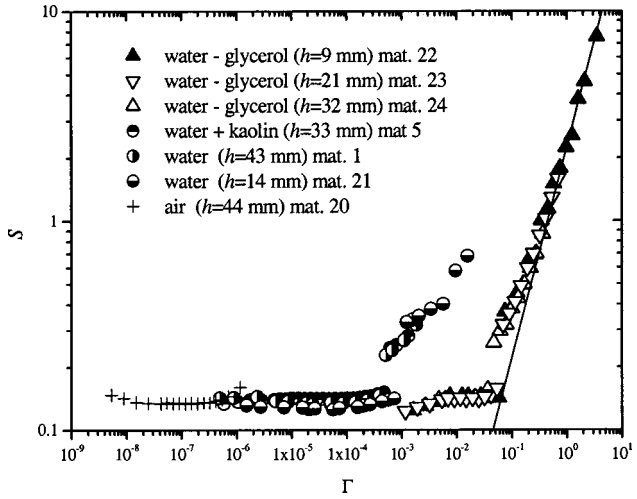

FIG. 1. Variation of the dimensionless shear stress S as a function of the dimensionless number Γ. The line drawn has a slope of 1($S \propto \Gamma$).

here. The experimental procedure was the same as the one presented here (see below). A transition in the bulk behavior can be observed at a critical value Γ ranging from 10^{-3} to 10^{-1} depending on the interstitial fluid viscosity. When $\Gamma \ll 1$, bulk behavior was typically frictional, namely, the shear stress was independent of the shear rate and varied linearly with the normal stress. Conversely, when $\Gamma \gg 1$, bulk behavior is typically Newtonian, namely, the shear stress is proportional to the shear rate. The authors interpreted their experiments as follows. When $\Gamma \ll 1$, the buoyant force outweighed the lubrication force and thus particles chiefly experienced direct frictional contacts. When $\Gamma \gg 1$, the fluid viscous force was sufficiently high to hinder any direct contact between particles. They then interact with each other only via hydrodynamic forces.

A similar dimensionless number may be built to estimate the relative importance of the viscoplastic lubrication force compared to the buoyant force when the behavior of the interstitial fluid surrounding coarse particles is no longer Newtonian but viscoplastic. The main issue is that there is no analytical expression of this force. Some experimental results suggest that it can vary as $\tau_c(\epsilon a)^{-2/3}$ [Ancey and Jorrot (2001)]. To evaluate the magnitude of the squeezing force of an interstitial viscoplastic fluid, we consider two coarse particles at rest. As is usual [Doraiswamy *et al.* (1991)], we assume that, before yielding, a viscoplastic material behaves as a Hookean elastic solid and that yielding can be described using a von Mises criterion (yielding when the second stress invariant exceeds τ_c). The maximum compression due to the buoyant force is $4\rho' ga/3$. The maximum compression that the elastoplastic medium can bear before yielding is $2\tau_k$. Therefore we can introduce a dimensionless parameter defined as the ratio of the buoyant force to the yield strength,

$$N = \frac{2}{3}\frac{\rho' ga}{\tau_k}. \tag{4}$$

For contact between two neighboring beads to be direct, the (buoyant) force due to gravity must exceed the strength resulting from plasticity. Thus it is expected that, for $N \gg 1$, contacts between coarse particles are direct while for $N \ll 1$ they are lubricated by the interstitial viscoplastic fluid.

TABLE I. Characteristics of the material employed in our tests. The values given for the yield stress were experimentally determined. For material 20, the interstitial fluid was air. For material 21, the interstitial fluid was water. For materials 22, 23, and 24, the interstitial fluid was a 98.5 glycerol/water solution.

Group	Material	ϕ_k	ϕ_c	ϕ_t	N	τ_c (Pa)	h (mm)
1	1	0.0	61.3	61.3	⋯	0	43
	2	0.0	61.3	61.3	20.6	0.1	32
	3	0.7	61.2	61.4	17.3	0.1	32
	4	1.3	61.0	61.5	14.8	0.2	32
	5	2.0	60.9	61.6	12.4	0.2	34
	6	2.6	60.7	61.7	10.7	0.2	32
	7	3.2	60.6	61.8	9.1	0.2	33
	8	4.0	60.4	62.0	7.5	0.3	33
	9	4.8	60.2	62.1	6.1	0.4	33
	10	5.5	60.0	62.2	5.1	0.4	33
	11	6.4	59.8	62.3	4.1	0.5	33
2	12	7.2	59.6	62.5	3.3	0.6	34
	13	8.2	59.3	62.6	2.5	0.8	34
	14	9.0	59.1	62.8	2.1	1.0	34
	15	9.8	58.9	62.9	1.7	1.2	35
3	16	11.4	58.5	63.2	1.1	1.7	35
	17	11.9	54.5	59.9	0.9	1.9	35
	18	15.4	47.9	55.9	0.3	4.5	60
	19	17.4	44.9	54.5	0.2	7.2	53
Miscellaneous	20	0	61	61	⋯	0	44
	21	0	61	61	⋯	0	14
	22	0	60	60	⋯	0	9
	23	0	60	60	⋯	0	21
	24	0	60	60	⋯	0	32

In summary, we infer from the above discussion that the bulk behavior of a bimodal concentrated suspension depends on the following dimensionless groups: ϕ_k, Pe_k, ϕ_c, N, and Γ. If we introduce a dimensionless shear stress $S = \tau/(\bar{\rho} gh)$, this means that we must have for a simple shear experiment $S = S(\Gamma, N, \phi_k, \phi_c, Pe_k)$. In the following, we also introduce a total solid concentration ϕ_t defined as $\phi_t = (V_c + V_k)/(V_c + V_k + V_w)$. The resulting bulk density is $\bar{\rho} = \phi_c \rho_c + (1-\phi_c)[\phi_k \rho_k - (1-\phi_k)\rho_0]$, where ρ_0 is the interstitial fluid density. The buoyant density is $\rho' = \phi_c[\rho_c - (\phi_k \rho_k + (1-\phi_k)\rho_0)]$. As reduced time, we use $\tilde{t} = t\Omega$, where Ω is the vane rotational velocity (see below).

IV. EXPERIMENTAL PROCEDURE

A. Materials

Nineteen mixtures of glass beads and kaolin with different solid concentrations were prepared. Table I summarizes the ingredients of each tested suspension. The kaolin concentration ranges from 0% to 17.4%. The glass–particle concentration ranged from 45% to 61.3%. The upper limit was very close to the maximum solid concentration for a uniform-particle suspension $\phi_{c,m} = 0.635$. Furthermore, five suspensions were prepared with water, air, or a 98.5% glycerol/water solution as interstitial fluid. The average solid concentration ranged from 0.6 to 0.61. The 98.5% glycerol/water solution had a density of 1260 kg/m^3. Its viscosity was evaluated at 0.96 Pa s (at 16 °C).

For the coarse fraction, we used calibrated glass beads provided by Verre Industrie (Marne-la-Vallée, France). The radius (a) was 0.4 mm. The particle density ρ_c was 2460 kg/m^3.

For the fine fraction, we used natural kaolin clay provided by Silice et Kaolin and Prolabo (France, Hostun). The particle density was approximately 2650 kg/m^3. The chemical composition was kaolin ($Al_2O_3.2SiO_2.2H_2O$) 99.84%, calcium 0.025%, chloride 0.025%, sulfate 0.0025%, and organic impurities 0.1%. The grain-size distribution was measured using a Malvern laser granulometer (see Sec. IV B for particulars). The volume median diameter of the particles was estimated to be 5.5 μm. The relatively large mean particle size was approximately 1–20 times greater than the expected size of an individual particle (a plate-like rigid aluminosilicate particle, whose typical size ranges from 0.3 to 2 μm) indicating that the dispersion was weakly flocculated. For our tests, the dispersion pH ranged from 7.3 to 7.9 in water and was around the value ($p\mathrm{H} \approx 7.5$) corresponding to the particle isoelectric point (neutrality of the double layer surrounding the particles) [Huifang, Low, and Bradford (1991); Lagaly (1989); Melton and Rand (1977)].

For each test, we prepared a clay dispersion by adding a given volume of kaolin to clear water. The dispersion was then vigorously mixed by hand for more than 20 min. The rheological characteristics of the dispersions were investigated using a Haake controlled-rate rheometer with parallel plate geometry (gap: 3 mm, radius: 25 mm). The plate surfaces were roughened with fine sand paper (equivalent diameter of 0.2 mm). As is usual for this kind of material [Coussot (1995); Coussot and Piau (1994)], we used a Herschel–Bulkley model to fit experimental data and estimate the yield stress:

$$\tau = \tau_k + K\dot{\gamma}^n. \tag{5}$$

The yield stress (τ_k) is an increasing function of the solid concentration ϕ_k. A theoretical model such as the one proposed by Zhou *et al.* (1999) can serve as a fit to the experimental data for sufficiently large solid concentrations [see Eq. (1)]. Using the least-square method to fit the data, we found $\kappa/(2a_k)^2 = 11\,585$ and $c = 5.15$. The uncertainty of the yield stress measurement was estimated at less than 10%. Moreover we found that $n \approx 0.35$, whatever the solid concentration.

B. Experimental setup and procedure

To measure the size distribution of fine particles, we used a Malvern laser granulometer which records particle populations within the range of 0.1–600 μm. Different procedures were used to test the measurement sensitivity. For instance, to limit flocculation, ultrasonic waves and an antiflocculation agent (a 5% sodium-hexametaphosphate solution) were used. For the materials tested, these two methods did not significantly change the particle-size distribution (we observed deviation of less than 20%). Moreover, for kaolin, we compared the results obtained with the laser granulometer with those given by the usual sedimentation test (as described in the French standard AFNOR NF P 94-068). Deviation in the mean size estimation between the two was less than 5%.

Determining the rheological properties of particle suspensions is somewhat difficult due to the presence of the coarse fraction. We therefore used a vane-shear cell. This involved equipping the Haake Rotovisco MV5 rheometer with a four-blade vane centered around a vertical shaft. The blade was 30 mm in radius (R_1) and 60 mm in height. The cell was 55 mm in radius (R_2) and 90 mm in depth, with smooth walls. Another cell with a radius of 100 mm was also used to detect any wall influence (for the frictional regime). This technique, used for soil mechanics, is now used increasingly in the rheometry of

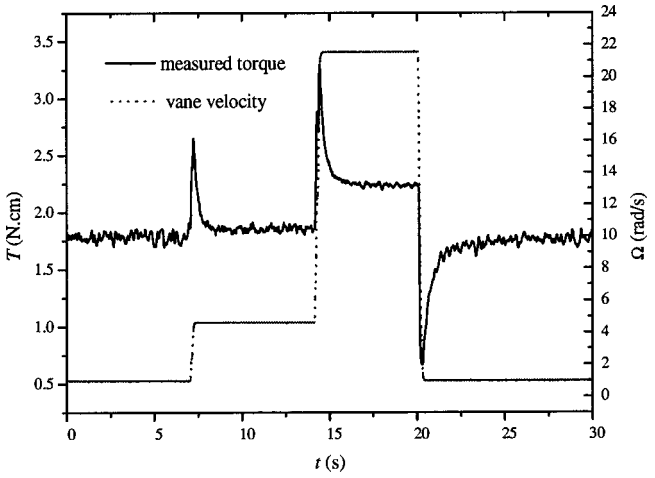

FIG. 2. Step change in rotational velocity and its effect on the measured torque. Data were collected at a sample rate of 50 Hz for material 5.

suspensions. Compared to conventional geometries, it gives more accurate results. With the material being trapped in the blades, shear is achieved around a fictive cylinder within the material. Problems such as depletion or slipping that, occur with (even roughened) metallic surfaces are avoided or at least attenuated. A shear vane has been used mainly for measuring the yield stress of concentrated suspensions: fine powders [Benarie (1961)], grease [Keentok, Milthorpe and O'Donovan (1985)], cement slurries [Keating and Hannant (1989)], thixotropic clay dispersions [Alderman, Meeten and Sherwood (1991)], red mud suspensions [Nguyen and Boger (1985); Nguyen and Boger (1983)], bead-glycerol suspensions [Ancey and Coussot (1999a)], pigment suspensions [Liddell and Boger (1996)], and emulsions [Yoshimura *et al.* (1987)]. Acceptable agreement has generally been found when the vane method was compared to other usual methods. Only on rare occasions has the suitability of the vane as a rheometer been addressed. On the basis of both experimental and numerical experiments, Barnes and Carnali (1990) found that, for sufficiently shear-thinning fluids, the vane provided better rheological data than the conventional Couette rheometer. Further numerical simulations performed by Yan and James (1997) supported this same conclusion for fluids with a yield stress.

As there are few experiments on this issue, we performed preliminary tests on a (Newtonian) 98.5% glycerol/water solution, then on a water–kaolin dispersion (at different solid concentrations) to obtain further insight into the rheometrical capacities of the vane [Ancey (1997)]. Comparison was made with parallel-plate and Couette rheometers as well as with simple tests indicated in the review on yield-stress measurement by Nguyen and Boger (1992). For the former material, the deviation between the rheometrical measurement obtained using various methods lay within a 2% range. For the latter, deviation as high as 15% was found. This was comparable to the deviation obtained by Liddell and Boger (1996) with TiO_2 suspensions (13%). Although severe, such deviation was within the current boundaries of acceptable uncertainty for rheometrical measurement in the present context.

For each tested material, the experimental procedure was as follows. The vane spindle was gently inserted into the material sample poured in the cell. The material depth was measured with uncertainty of less than 1%. The vane was then rotated at a given speed and we recorded the torque-time response measured by the torque transducer of the

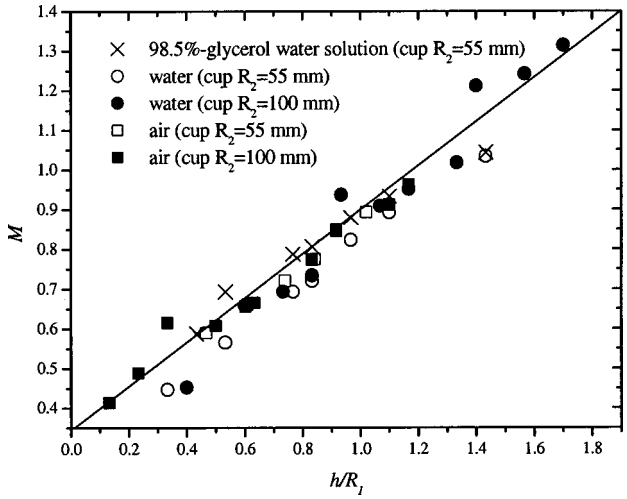

FIG. 3. Variation in the dimensionless torque M (measured for $\Omega = 0.2$ rad/s) as a function of the ratio h/R for concentrated suspensions of glass beads ($a = 0.4$ mm, $\phi_c = 0.61$) within different interstitial fluids. Variation in the dimensionless torque M (measured for $\Omega = 0.2$ rad/s) as a function of the ratio h/R for concentrated suspensions of glass beads ($a = 0.4$ mm, $\phi_c = 0.61$) within different interstitial fluids.

rheometer with a sampling rate ranging from 1 to 50 Hz. For each test, the torque progression was measured for a period ranging from 5 to 30 min. After this test, the sample was left at rest for a few minutes, then a new velocity was selected. Step changes in applied rotational velocity and loop tests were also performed to detect possible time effects on bulk behavior. Figure 2 shows the typical mechanical response of a tested suspension as a result of step changes.

Unlike the Couette rheometer, for which end effects (friction on the cylinder underside) can be easily reduced, there is no practical solution for the vane as far as we know. The end effects were estimated by measuring the dependence of the torque on the immersed depth. This method should give more accurate results than its estimate obtained from a speculative computation of the shear distribution over the vane underside (see [Nguyen and Boger (1985)]). The resulting torque can be split into two contributions,

$$T = T_s + T_e. \tag{6}$$

The first ($T_s = 2\pi h R_1^2 \tau$) corresponds to the shearing on the imaginary cylinder around the vane blades. The second ($T_e = 2\pi \int_0^{R_1} r^2 \tau dr$) pertains to the shearing on the vane imaginary circular underside. For simple fluids, the shear stress τ acting on a surface does not depend on the normal stress σ and thus on the depth. In this case, the resulting torque must be a linear function of the flow depth. The underside contribution T_e is then determined as the intercept at $h = 0$ in the plot of T vs h (for a fixed value of Ω). For complex fluids, the nondependence of τ on σ may fail. In the present case in which granular materials were used, frictional contacts at the particle level involve the linear dependence of τ on σ (Coulombic behavior) at the macroscopic scale. The primary torque contribution T_s is expected to be a square function of the immersed height while the underside contribution is a linear function. The end effect is thus estimated as the intercept of the dimensionless torque $M = T/(\pi \rho' g h R_1^3)$ vs h/R (still for a fixed value of Ω). Figure 3 shows the variation of M vs h/R for material 5. Here, within the range of our experi-

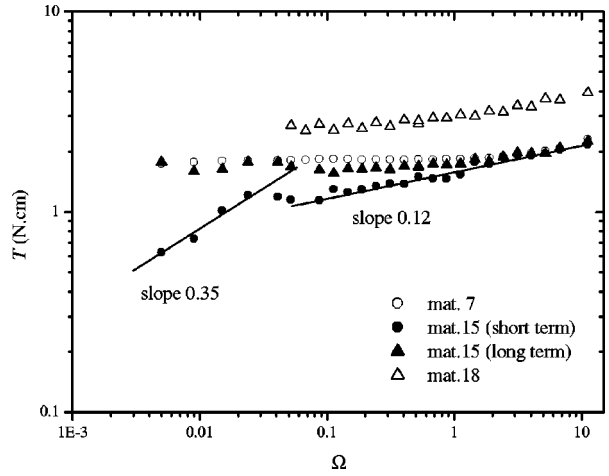

FIG. 4. Variation in the torque T as a function of the rotational speed of the vane Ω for three materials. For material 15, the mechanical response depends on the time.

ments, we found $T_s = T/[1+2R_1/(3mh)]$, with $m = 0.54$ for the frictional behavior and $m = 2$ for the viscous behavior. The shear stress can be then directly computed as follows: $\tau = T_s/(2\pi hR_1^2)$.

In an attempt to link shear stress to shear rate, we computed the shear rate from the torque-speed data. Specific attention must be paid to the use of this procedure since many complications may disturb results for non-Newtonian fluids. First, at low shear rates (i.e., when determining the yield stress), the data reduction is very sensitive to noise and the kind of interpolation used. Then, as indicated by Nguyen and Boger (1992) in the case of yield stress fluids, correction to the usual Krieger method must be made to account for the yield surface when the material is partially sheared, i.e., at low rotational speed. For granular material in a frictional regime, we observed that shear was concentrated within a narrow annulus around the inner cylinder, whose thickness only slightly exceeded 10 particle diameters. In the following presentation of experimental data, due to uncertainty in the computation of the shear rate, we prefer to replace it with the rotational velocity of the vane in the definition of the dimensionless number Γ [Eq. (3)]. Moreover, Γ depends on the mean particle-to-particle distance ϵa. This reduced distance ϵ is usually computed as

$$\epsilon = 2\left[1-\left(\frac{\phi_c}{\phi_{c,m}}\right)^{1/3}\right]\left(\frac{\phi_c}{\phi_{c,m}}\right)^{-1/3}. \tag{7}$$

V. EXPERIMENTAL RESULTS AND COMMENTS

The observed behavior was quite complex and is, probably, best explained by describing the typical flow pattern. To that end, we have split our results into three distinctive groups. Figure 4 gives typical variations of the measured torque as a function of the rotational speed for each group. Group 1, including materials 1–11, shall be referred to as the *frictional group*. Group 2, comprising materials 12–15, is the more complex, exhibiting time-dependent properties and various mechanical responses. Here it will be denoted the *intermediate group*. Finally, group 3, comprising tests 16–20, shall be called *viscoplastic*.

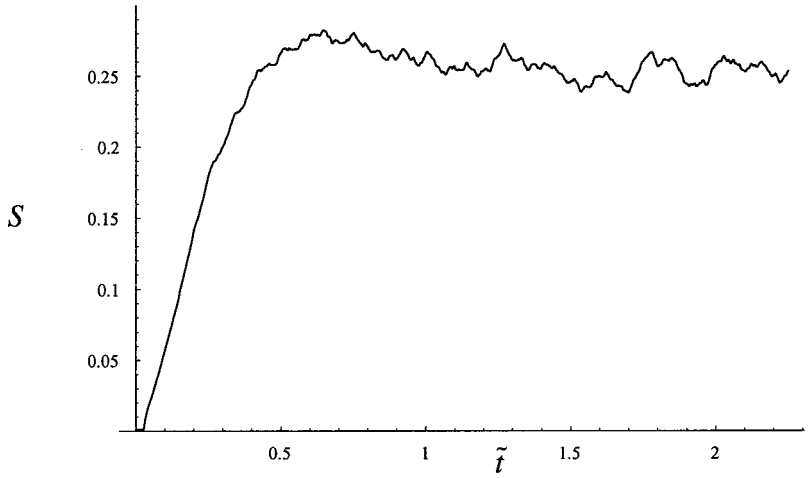

FIG. 5. Variation in the dimensionless shear stress S with time for material 5 sheared at a velocity of 0.005 rad/s.

A. Group 1 materials

For group 1 materials, the solid concentration in glass beads ranged from 59.8% to 61.3% while the concentration in kaolin was lower than 6.4%. For this group, the dimensionless number N ranged between approximately 4 and 21. In Fig. 4, a noticeable change in bulk behavior can be seen, depending on the rotational speed. At low velocities, the torque T_s was found to be a quadratic function of the flow depth and to be independent of the rate (see Fig. 3). Observation of the free surface suggested that shear was localized within a narrow band around the vane. At high rates, the torque varied linearly with the vane velocity and the flow depth. The suspension contained in the cell was fully sheared. In terms of stress, this means that a frictional (Coulombic) regime occurred at low rates while a viscous (Newtonian) regime took place for high vane velocities. When the material was set in motion, the steady state was reached after a short time: $\tilde{t} \approx 1$ (see Fig. 5), with a smooth, regular increase in stress. When step changes in the rotational velocities were applied (see Fig. 2), the steady state was preceded by a sharp, rapid increase (decrease) in stress when the shear velocity was suddenly raised (diminished).

In a previous paper [Ancey and Coussot (1999a)], we suggested the following explanation. Because at low rotational rates frictional contacts between particles predominate ($\Gamma \ll 1$), at the macroscopic scale, it is natural to find Coulombic behavior. For larger velocities ($\Gamma \ll 1$), viscous forces are able to break direct contacts and lubricate them. Once most contacts are lubricated, one can expect viscous behavior on the macroscopic scale, as is usual for hard-sphere suspensions (see Fig. 1). Here the transition arose for values of the dimensionless rotational speed of Γ close to 10^{-3} but it was markedly less pronounced than for bead suspensions in glycerol/water solution. In the latter case, experimental data collapsed rapidly on the curve $S \propto \Gamma$ (see Fig. 1) while in the former the corresponding data fell onto the curve $S \propto \Gamma^{1/3}$. It is expected that at high-shear velocities, they joined the curve $S \propto \Gamma$ but this was not achieved in the range of our tests.

A closer examination of torque fluctuations shows that a change in bulk behavior occurred also for lower values of Γ, as shown in Fig. 6. For a dimensionless rotational speed lower than 10^{-4}, we measured a fluctuating signal for the torque, with a relative magnitude of fluctuations around 4% and independent of the rotational speed. For a

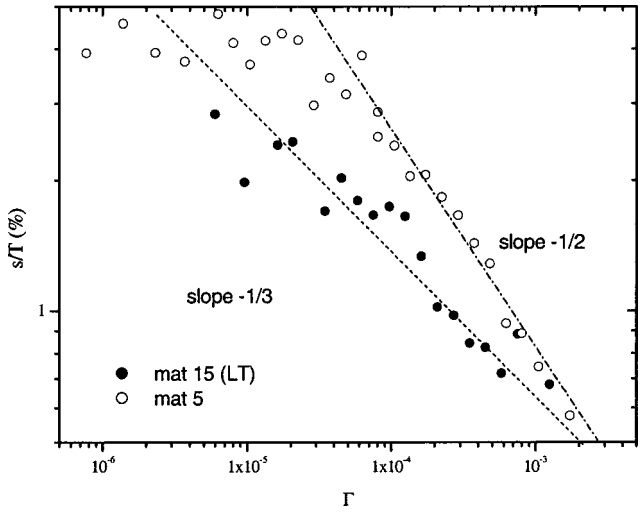

FIG. 6. Variation in the standard deviation s of the recorded signal T as a function of the rotational speed Γ.

rotational speed in excess of 10^{-4}, the fluctuation amplitude decreased for increasing rotational speeds. Both the fluctuation amplitude and standard deviation of recorded signals decreased as $\Gamma^{-1/2}$. The decrease in the fluctuation strength was probably due to the damping action of lubricated contacts. Such decay contrasts with available theoretical predictions. For instance, Phan-Thien's (1995) model predicts that the strength of fluctuations varies as Γ. The change in the fluctuation behavior may be explained as follows. At low-shear velocities, particles were linked together via a force network. Shearing induced the creation and breakdown of several force chains [Aharonov and Sparks (1999)], generating fluctuations on a large scale. A particle experiencing frictional contacts bore a large part of the weight of the above particle column and therefore the fluctuation strength was expected to be significant and independent of the shear velocity. When contacts were increasingly lubricated with increasing shear velocities, the gravity force ceased being transmitted from upper to lower layers. This led to a decrease in the force supported by the particles. In parallel, since chains of forces were broken, force fluctuations could not be transmitted throughout the network and conversely could be damped by the interstitial fluid separating particles.

B. Group 2 materials

For group 2 materials, the solid concentration in glass beads ranged from 62.5% to 62.9% while the concentration in kaolin ranged from 7.2% to 9.8%. For this group, the dimensionless number N ranged from 1.7 to 3.3. The major difference from group 1 materials is that the steady state was reached after a fairly long time. For all the materials of this group tested, we observed that, once the material was set into motion, the shear stress varied towards its steady-state value in an irregular manner. Figure 7 illustrates the typical shear stress measured for a suspension belonging to group 2. Just after the onset of motion, at time $\tilde{t} = t_{\max} \approx 1$, the shear stress reached a maximum. Then a slow decrease to a minimum value was observed until time $\tilde{t} = t_{\min}$. Generally this minimum lasted several seconds. Since it took on the appearance of a stress plateau, it gave the impression that the steady state was achieved. But, after a given period, the shear stress continued rising to a constant value. For very long times $\tilde{t} \gg t_{\text{st.state}}$ (within the range of

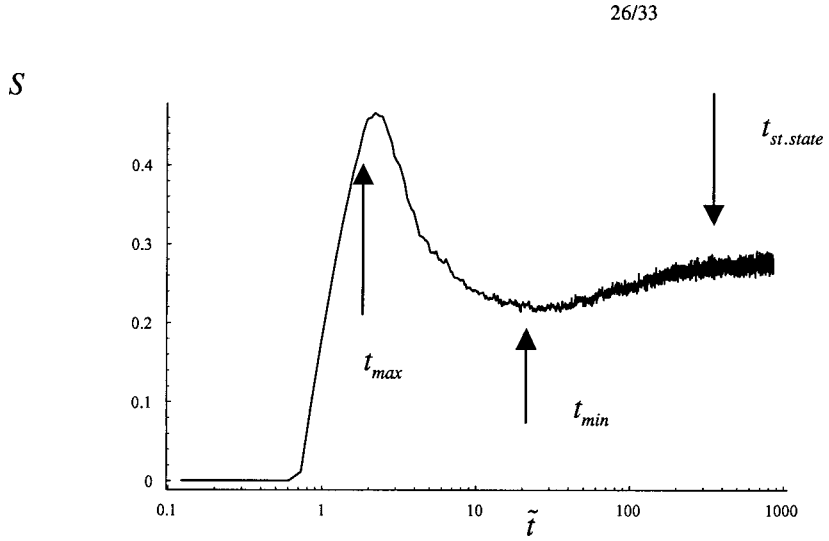

FIG. 7. Variation in the stress S vs time for material 15 sheared at a velocity of 0.243 rad/s.

tested times), the shear stress held a constant value. The three characteristic times that we have just introduced depended on the shear velocity. Figure 8 shows the variation of the three dimensionless characteristic times with the dimensionless shear velocity Γ. For shear velocities as high as 10^{-5}, the first characteristic time $t_{\max}$ associated with the maximum in shear stress is fairly constant. For Γ in excess of 10^{-5}, $t_{\max}$ increased linearly with Γ. The time $t_{\min}$ associated with the stress minimum was first a decreasing function of Γ($t_{\min} \propto \Gamma^{-1}$), then for Γ in excess of 10^{-4}, it tended toward a constant value. For high-shear velocities, $t_{\min}$ and $t_{\text{st.state}}$ had the same order. This also means that the steady-state plateau and the minimum in stress coincided. The existence of different

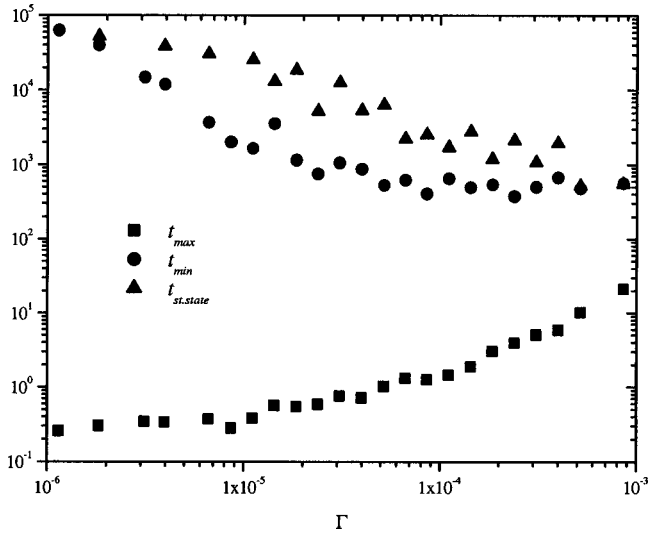

FIG. 8. Variation in the dimensionless characteristic times $t_{\max}$, $t_{\min}$, and $t_{\text{st.state}}$ as functions of the dimensionless shear velocity Γ for material 15.

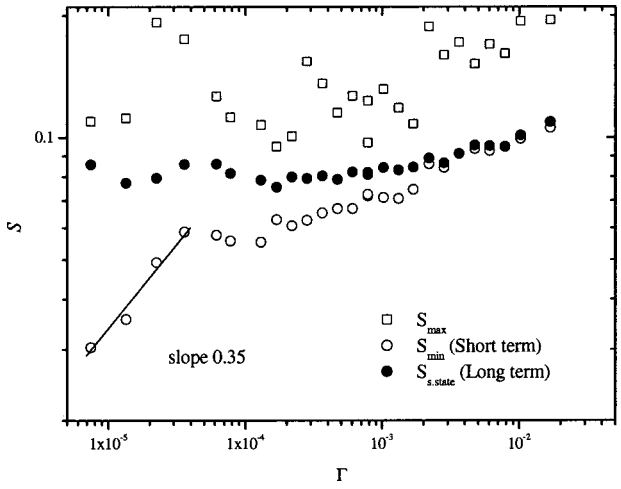

FIG. 9. Variation in the dimensionless shear stress computed for the three characteristic times ($t_{\max}$, $t_{\min}$, and $t_{\text{st.state}}$) as functions of the dimensionless shear velocity Γ for material 15.

characteristic times means that the stress response of the material depended on the characteristic duration of the deformation imposed on the material. It is then possible to distinguish between short-term mechanical behavior and long-term behavior. Figure 9 shows typical shear stress variation as a function of the shear velocity (material 15). It should be noted that, in the short-term response of the material, the dimensionless shear stress varied as a power function of the shear velocity. This means that the instantaneous effective behavior of the material was shear thinning and without apparent yield stress. In contrast with the short-term behavior, the long-term behavior was frictional viscous in a way similar to the group 1 materials. The same overall characteristics regarding the variation of the torque with the shear velocity were found again. Figure 6 gives the variation of the fluctuation strength as a function of the shear velocity. The main difference with group 1 materials is that the fluctuation strength varied as $\Gamma^{-1/3}$ rather than $\Gamma^{-1/2}$.

The specific behavior of materials belonging to group 2 probably reflects the change in the nature of the contact between particles. When the mixture was just stirred and poured into the shear cell, the gross particles were embedded in the colloidal dispersion. The particles were then generally separated by a thin layer of dispersion. Since the ratio N was close to 1, it can be expected that the buoyant force approximately balanced the resistance force exerted by the dispersion on the coarse particles due to the yield stress. As the settling velocity of coarse particles was small, direct contacts between coarse particles arose after a sufficiently long time only. This can explain why there were short-term and long-term behaviors. The short-term behavior correspond to a loose particle arrangement, in which most coarse particles were surrounded by the interstitial fluid. In this case, the dispersion imparted most of its rheological features to the suspension. As shown in Fig. 9, at least for sufficiently slow shear velocities, the bulk shear stress varied as $S \propto \Gamma^{0.35}$ in a way similar to the shear stress within the dispersion [see Eq. (5)]. The long-term behavior correspond to the development of a particle network within the bulk, responsible for frictional behavior. As for group 1 materials, the shear-velocity increase enhanced the interstitial fluid inertia and, for sufficiently large-shear velocities, contacts between coarse particles were lubricated by the dispersion.

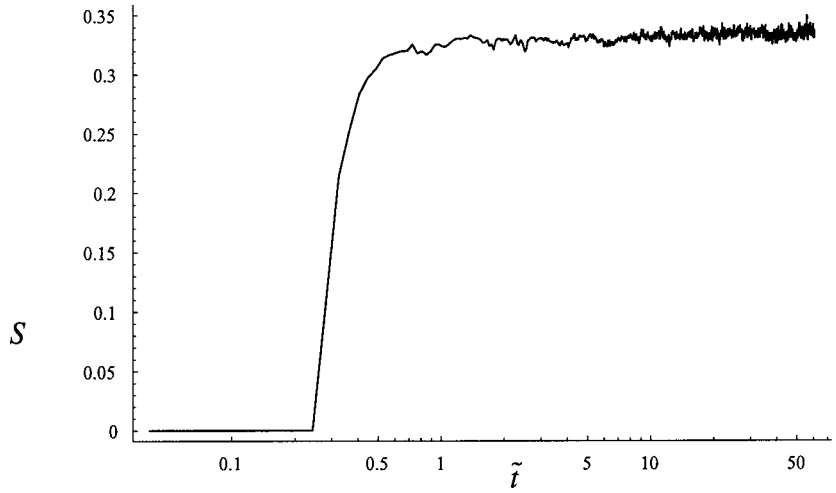

FIG. 10. Variation in the stress S with time for material 19 sheared at a velocity of 0.405 rad/s.

C. Group 3 materials

For group 3 materials, the solid concentration in glass beads ranged from 44.9% to 54.5% while the concentration in kaolin ranged from 11.4% to 17.4%. The dimensionless number N ranged from 0.2 to 1.1. For this group, the steady state was achieved very quickly after the material was set into motion (see Fig. 10). Reproducibility tests showed that, for the same material, from one test to another, the experimental curves S vs Γ did not define a single master curve but, on the contrary, formed a series of parallel curves (see Fig. 11). We then defined the bulk shear stress statistically by averaging the different values measured experimentally for a given shear velocity. The deviation between the experimental curves and the mean curve was as high as 20%. This deviation contrasts

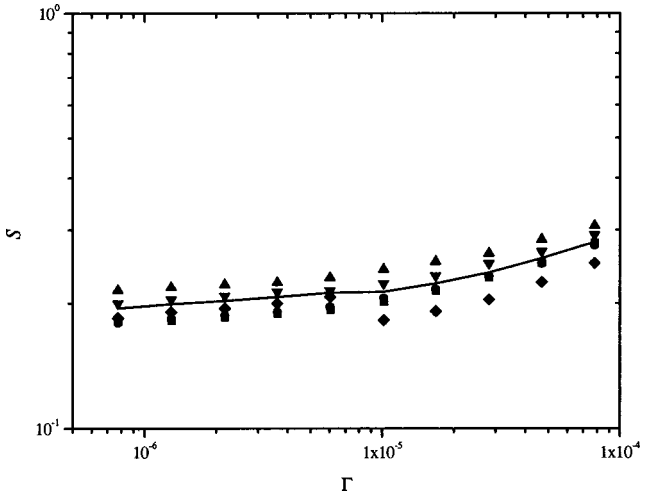

FIG. 11. Dimensionless flow curve obtained for material 19 during the reproducibility tests. The continuous curve represents the mean value computed by averaging the experimental curves.

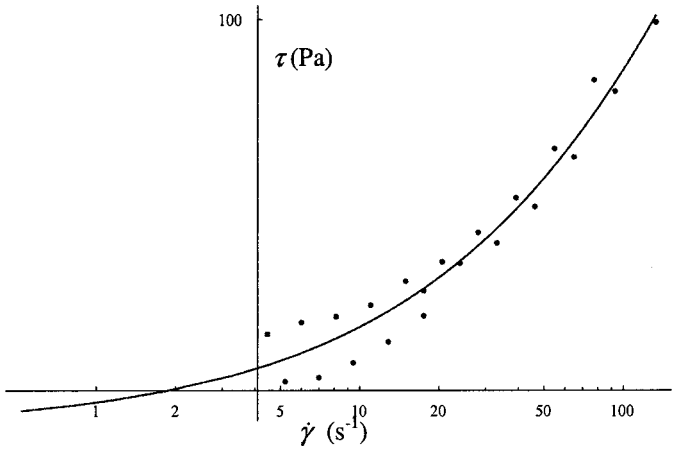

FIG. 12. Mean flow curve of material 18. The continuous curve represents the equation $\tau = 61 + 1.9\dot{\gamma}^{0.62}$, which was fitted on the mean experimental points. The points shown represent two series of experimental data (we have reported only the points farthest from the mean curve).

with the stress-fluctuation strength measured for a single test. Indeed, the fluctuation strength was low (typically s/T ranged from 0.4% to 1%) and did not depend on the shear velocity.

For group 3 materials, bulk behavior was clearly viscoplastic and it can be fairly well described using a Herschel–Bulkley model in the form of Eq. (1). Figure 12 shows a typical mean flow curve obtained using the method proposed by Nguyen and Boger [Nguyen and Boger (1992)] for computing the shear rate in the case of partially sheared flows. Using a built-in routine in Mathematica 4.0 software, we fitted experimental data using a Herschel–Bulkley model. Generally, we found that the exponent n for the bulk was much greater than the value found for the dispersion alone (0.6 instead of 0.35). This probably reflects a contribution from the coarse fraction in the energy dissipation (and thus in the viscosity rise). Moreover the bulk yield stress increased both with the kaolin and coarse-particle concentrations. As explained previously by other authors [Coussot and Piau (1995)], the bulk viscoplastic behavior was dictated by the interstitial fluid. Since the ratio N was near or less than 1, the interstitial-fluid resistance outweighed the buoyant force acting on the coarse particles. Thus most coarse particles were embedded in a colloidal matrix and experienced only viscoplastic forces.

VI. CONCLUDING REMARKS

This series of experiments clearly shows that the bulk rheological properties exhibited by concentrated suspensions of fine (colloidal) and coarse particles within a Newtonian fluid are various and controlled by at least two parameters. This diversity originates from the possibility of different interactions between coarse particles. When direct contact between coarse particles prevails and thus a network of particles in close contact takes place throughout the bulk, the suspension behavior is typically frictional. When contacts between coarse particles are lubricated by the interstitial fluid (the mixing of fine colloidal particles and the Newtonian fluid), the interstitial fluid imparts its rheological features to the bulk. Thus either Newtonian or non-Newtonian viscoplastic bulk behavior can be observed depending on the solid concentration in fine (colloidal) particles. Therefore it follows that the first approximation proposed by Sengun and Probstein is valid, provided that the coarse particles do not experience direct contact.

Moreover, each type of contact can be associated with a characteristic time, which can be defined as the time required for contact to be achieved. Depending on this characteristic time and on the time scale associated with the experiment, a time-dependent bulk behavior can be observed. For our experiments, this arose for group 2 materials, for which, at rest, the buoyant force acting on particles approximately balanced the plastic force exerted by the interstitial fluid. For this group, the frictional steady-state regime was reached only a long while after the material was set into motion. Indeed, for the particle network to form, almost all the coarse particles had to settle.

In the present context, the distribution in size included fine and gross particles and thus can be referred to as bimodal. The paramount features of the bulk behavior can be given using four dimensionless numbers: the solid concentrations in coarse and fine particles, respectively, ϕ_c and ϕ_k, the ratio of the buoyant force to the plastic force, $N = \rho' gR/\tau_k$, and a dimensionless shear velocity $\Gamma = \mu\Omega/(\epsilon\rho' gh)$, which can also be seen as the ratio of the buoyant to the viscous forces. When $N \gg 1$, contact between particles is not influenced by the yield stress of the interstitial fluid. In this case, the bulk behavior is either frictional ($\Gamma < 10^{-4}$) or viscous ($\Gamma > 10^{-4}$). When $N \to 1$, the bulk behavior is characterized by time-dependent properties, exhibiting shear-thinning properties in the short term and frictional properties in the long term. When $N < 1$, the bulk behavior is viscoplastic.

A direct application of the present results concerns the physics of debris flows in mountain areas. To explain the striking mobility of these natural flows involving a wide range of materials (fine sediment, boulders, etc.), geologists usually evoke the pore-fluid pressure as the key mechanism. In this article it was shown that a fluid-like state is reached for very concentrated slurries when contact between coarse particles is lubricated by the interstitial fluid. Such an explanation appears to the author to be better founded. Moreover, it should be possible to predetermine bulk behavior of natural slurries depending on its composition, at least in simple cases. This would be a result of primary importance in engineering.

ACKNOWLEDGMENTS

This study was supported by Cemagref and funding was provided by the Institut National des Sciences de L'Univers of the CNRS (PNRN 99 29 CT). The author is grateful to Dr. P. Coussot for helpful comments and to Professor P. Banfill and Dr. S. Mansoutre for interesting references.

References

Acrivos, A., R. Mauri, and X. Fan, ''Shear-induced resuspension in a Couette device,'' Int. J. Multiphase Flow **19**, 797–802 (1993).

Aharonov, E. and D. Sparks, ''Rigidity phase transition in granular packings,'' Phys. Rev. E **60**, 6890–6896 (1999).

Alderman, N. J., G. H. Meeten, and J. D. Sherwood, ''Vane rheometry of bentonite gels,'' J. Non-Newtonian Fluid Mech. **39**, 291–310 (1991).

Ancey, C., ''Rhéologie des écoulements granulaires en cisaillement simple,'' Ph.D. thesis, École Centrale de Paris, Châtenay-Malabry, France (1997).

Ancey, C. and P. Coussot, ''Transition from frictional to viscous regimes for granular suspensions,'' C. R. Acad. Sci. Paris Ser. II **327**, 515–522 (1999a).

Ancey, C. and H. Jorrot, ''Yield stress for particle suspensions within a clay dispersion,'' J. Rheol. **45**, 297–319 (2001).

Ancey, C., P. Coussot, and P. Evesque, ''A theoretical framework for very concentrated granular suspensions in a steady simple shear flow,'' J. Rheol. **43**, 1673–1699 (1999b).

Banfill, P. F. G., ''Rheological methods for assessing the flow properties of mortar and related materials,'' Constr. Build Mat. **8**, 43–50 (1994).

Banfill, P. F. G. ''The influence of fine materials in sand on the rheology of fresh mortar,'' in *Proceedings of the Utilizing of Ready Mix Concrete and Mortar*, edited by R. K. Dhir and M. C. Limbachiya (Telford, Dundee, UK, 1999), pp. 411–420.

Barnes, H. A. and J. O. Carnali, ''The vane-in-cup as a novel rheometer geometry for shear thinning and thixotropic materials,'' J. Rheol. **34**, 851–866 (1990).

Benarie, M. M., ''Rheology of granular material II—A method for the determination of the intergranular cohesion,'' Br. J. Appl. Phys. **12**, 514–518 (1961).

Coussot, P., ''Structural similarity and transition from Newtonian to non-Newtonian behavior for clay-water suspensions,'' Phys. Rev. Lett. **20**, 3971–3974 (1995).

Coussot, P., *Mudflow Rheology and Dynamics* (Balkema, Rotterdam, 1997).

Coussot, P. and C. Ancey, ''Rheophysical classification of concentrated suspensions and granular pastes,'' Phys. Rev. E **59**, 4445–4457 (1999).

Coussot, P. and J.-M. Piau, ''On the behavior of fine mud suspensions,'' Rheol. Acta **33**, 175–184 (1994).

Coussot, P. and J.-M. Piau, ''The effects of an addition of force-free particles on the rheological properties of fine suspensions,'' Can. Geotech. J. **32**, 263–270 (1995).

Doraiswamy, D., A. N. Mujumdar, I. Taso, A. N. Beris, S. C. Danforth, and A. B. Metzner, ''The Cox–Merz rule extended: A rheological model for concentrated suspensions and other materials with a yield stress,'' J. Rheol. **35**, 647–685 (1991).

Huifang, Z., P. F. Low, and J. M. Bradford, ''Effects of *p*H and electrolyte concentrations on particle interaction in three homoionic sodium clay suspensions,'' Soil Sci. **151**, 196–207 (1991).

Husband, D. M., N. Aksel, and W. Geissle, ''The existence of static yield stresses in suspensions containing noncolloidal particles,'' J. Rheol. **37**, 215–235 (1993).

Jomha, A. I., A. Merrington, L. V. Woodcock, H. A. Barnes, and A. Lips, ''Recent developments in dense suspension rheology,'' Powder Technol. **65**, 343–370 (1990).

Jongshaap, R. J. J. and J. Mellema, ''Stress tensor expressions for dispersions,'' J. Rheol. **39**, 953–959 (1995).

Kapur, P. C., P. J. Scales, B. V. Boger, and T. W. Healy, ''A theoretical framework for the yield stress of suspensions loaded with size distributed particles,'' AIChE J. **43**, 1171–1179 (1997).

Keating, J. and D. J. Hannant, ''The effect of rotation rate on gel strength and dynamic yield strength of thixotropic oil well cements measured using a shear vane,'' J. Rheol. **33**, 1011–1020 (1989).

Keentok, M., J. F. Milthorpe, and E. O'Donovan, ''On the shearing zone around rotating vanes in plastic liquids: Theory and experiment,'' J. Non-Newtonian Fluid Mech. **17**, 23–35 (1985).

Krieger, I. M., ''Rheology of monodispersed lattices,'' Adv. Colloid Interface Sci. **3**, 111–136 (1972).

Kytömaa, H. K. and D. Prasad, ''Transition from quasi-static to rate dependent shearing of concentrated suspensions,'' in *Powders and Grains*, edited by C. Thornton (Balkema, Rotterdam, 1993), pp. 281–287.

Lagaly, G., ''Principles of flow of kaolin and bentonite dispersion,'' Appl. Clay Sci. **4**, 105–123 (1989).

Liddell, P. V. and D. V. Boger, ''Yield stress measurements with the vane,'' J. Non-Newtonian Fluid Mech. **63**, 235–261 (1996).

Mansoutre, S., ''Des suspensions concentrées aux milieux granulaires lubrifiés: Étude des pâtes de silicate tricalcique,'' Ph.D. thesis, Université d'Orléans, Orléans, France, 2000.

Mansoutre, S., P. Colombet, and H. Van Damme, ''Water retention and granular rheological behavior of fresh C3S paste as a function of concentration,'' Cem. Concr. Res. **29**, 1441–1453 (1999).

Melton, I. E. and B. Rand, ''Particle interactions in aqueous kaolinite suspensions,'' J. Colloid Interface Sci. **60**, 308–336 (1977).

Nguyen, Q. D. and D. V. Boger, ''Yield stress measurement for concentrated suspensions,'' J. Rheol. **27**, 321–349 (1983).

Nguyen, Q. D. and D. V. Boger, ''Direct yield stress measurement with the vane method,'' J. Rheol. **29**, 335–347 (1985).

Nguyen, Q. D. and D. V. Boger, ''Measuring the flow properties of yield stress fluids,'' Annu. Rev. Fluid Mech. **24**, 47–88 (1992).

Phan-Thien, N., ''Constitutive equation for concentrated suspensions in Newtonian liquids,'' J. Rheol. **39**, 679–695 (1995).

Russel, W. B., ''Review of the role of colloidal forces in the rheology of suspensions,'' J. Rheol. **24**, 287–317 (1980).

Russel, W. B., D. A. Saville, and W. R. Schowalter, *Colloidal Dispersions* (Cambridge University Press, Cambridge, 1995).

Scales, P. J., P. C. Kapur, S. B. Johnson, and T. W. Healy, ''The shear yield stress of partially flocculated colloidal suspensions,'' AIChE J. **44**, 538–544 (1998).

Sengun, M. Z. and R. F. Probstein, ''Bimodal model of slurry viscosity with applications to coal slurries. Part 1. Theory and experiment,'' Rheol. Acta **28**, 382–393 (1989).

Terzaghi, K., *Theoretical Soil Mechanics* (Wiley, New York, 1943).

van den Brule, B. H. A. A. and R. J. J. Jongshaap, ''Modeling of concentrated suspensions,'' J. Stat. Phys. **62**, 1225–1237 (1991).

van der Werff, J. C. and V. F. de Kruif, ''Hard-sphere colloidal dispersions: The scaling of rheological properties with particle size, volume fraction, and shear rate,'' J. Rheol. **33**, 421–454 (1989).

Wildemuth, C. R. and M. C. Williams, ''Viscosity of suspensions modeled with a shear-dependent maximum packing fraction,'' Rheol. Acta **23**, 627–635 (1984).

Wildemuth, C. R. and M. C. Williams, ''A new interpretation of viscosity and yield stress in dense slurries: Coal and other irregular particles,'' Rheol. Acta **24**, 75–91 (1985).

Yan, J. and A. E. James, ''The yield surface of viscoelastic and plastic fluids in a vane viscometer,'' J. Non-Newtonian Fluid Mech. **70**, 237–253 (1997).

Yoshimura, A. S., R. K. Prud'homme, H. M. Princen, and A. D. Kiss, ''A comparison of techniques for measuring yield stress,'' J. Rheol. **31**, 699–710 (1987).

Zhou, Z., M. J. Solomon, P. J. Scales, and D. V. Boger, ''The yield stress of concentrated flocculated suspensions of size distributed particles,'' J. Rheol. **43**, 651–671 (1999).